First principles calculation of configurational energy density of states for LLTO with new Wang and Landau algorithm variant

Jason D. Howard[1]

[1]*Materials Science Division, Argonne National Lab, Lemont, IL, 60439, USA*
(Dated: January 7, 2020)

In this work a variant of the Wang and Landau algorithm for calculation of the configurational energy density of states is proposed. The algorithm was developed for the purpose of working towards the goal of using first principles simulations, such as density functional theory, to calculate the partition function of disordered sub lattices in crystal materials. The expensive calculations of first principles methods make a parallel aglorithm necessary for a practical compuation of the configurational energy density of states within a supercell approximation of a solid state material. The developed algorithm is natural to paralleize, is developed from a self consistent perspective, and was developed purposely for lattice based problems encountered in the study of disordered crystal sublattices. The algorithm develped in this work is tested with the 2d Ising model to bench mark the algorithm and to help provide insight for implementing the algorithm to a materials science application. The algorithm is then applied to the lithium and lanthanum sublattice of the solid state lithium ion conductor $Li_{0.5}La_{0.5}TiO_3$. This was done to help understand the disordered nature of the lithium and lanthanum. The results find overall that the algorithm performs very well for the 2-d Ising model and that the results for $Li_{0.5}La_{0.5}TiO_3$ are consistent with experiment while providing additional insight into the lithium and lanthanum ordering in the material.

INTRODUCTION

For crystalline materials with disordered sub-lattices such as the Li-ion solid state electrolyte LLTO it is desirable to calculate from first principles methods(such as density functional theory[1]) the configurational energy density states $G(E_j)$. Here the energy density of states refers to the energies of the distinct lattice configurations. With the energy density of states the partition function,

$$Z = \sum_{i}^{\Omega} e^{\frac{-e_i}{k_B T}} = \sum_{j}^{\Pi} G(E_j) e^{\frac{-E_j}{k_B T}} \ , \qquad (1)$$

can be determined and from it many important thermodynamics properties such as the free energy, entropy, specific heat, and ensemble averages calculated. In Eq. (1), Ω corresponds to the number of possible configurations and energies in the set $\{\Sigma_i, e_i\}_\Omega$, Π to number of possible distinct energies E_j, k_B is Boltzman's constant, and T is the temperature. One method to solve this problem could be temperature dependent simulations involving the Metropolis algorithm an sampling with probality proportional to $exp(\frac{-e_i}{k_B T})$ and histogram re-weighting techniques[2, 3]. Another more adanved method is the multi-canonical method proposed by Berg et al. [4]. A variant of multicanaonical sampling that samples the density of states directly known as entropic sampling developed by Lee [5] could also be used. These algorithms require a good estimate of the density of states to be effective. Another algorithm called the Wang and Landau algorithm [6] has been developed which is temperature independent and is based on a random walk in energy space and builds up the density of states as the algorithm progresses. An issue with these algorithms(if using a single walker) in use with first principles methods such as

density functional theory is the large number of iterations needed which would require a prohibitively long wall time at the current performance power of computers. In this paper an algorithm is proposed that combines the use of random sets along with the importance sampling method of the Wang and Landau algorithm, this importance sampling is similar to the entropic sampling proposed by Lee [5]. The algorithm also used the philosophy of the Wang and Landau algorithm to build up a estimate of the density of states as the algorithm progresses. The proposed algorithm is meant to work towards the goal of a highly parallel importance sampling algorithm that directly calculates the density of states, meshes well with high performance computing architectures, and has a minimum of parmaters for implementation. The algorithm developed in this work is referred to as the B_LENDER ($B_L$end Each New Density Each Round) algorithm.

The Wang and Landau method does have parallel versions, including restricting random walkers to specific energy ranges or allowing the walkers to explore the entire space while periodically communicating with each other [7–9]. The B_LENDER algorithm is charecterized by allowing the walkers to expore the entire energy range and communication with each other through an update to the density of states at each iteration. There also have been reports of the Wang and Landau algorithm used with first principles calculations to calculate magnetic properties of materials and order to disorder properties of alloys by [10, 11]. In principle many of the different forms of the Wang and Landau sampling currently used are based around the concept of sampling until a flat historgram of the visted energies is reached followed by a reduction in the modification factor of the density of states. There have been advancements made in understanding how to

reduce the modification factor by Belardinelli et al. [12] whom developed the 1/t algorithm, this result was verified by the work of Zhou et al. [13]. The novel aspects of the B_LENDER algrotihm include, a continuous adapation of the modification factor to the density of states using the current sum of the density of states as a regulator, using the number of configurations as an parameter in the modification factor, and using a histogram of the currently visited energies/configurations as a parameter in the modification factor. The algorithm in this work was also formulated in a self consistent fashion, is believed to naturally evolve to a flat histogram of the visted energy levels, and is natural to parallelize as it is based on a set of random walkers. The algorithm is not claimed to supercede or be superior to other variants of the Wang and Landau algorithm but was developed purposely for ease of use in the application to disorered sublattices of crystal systems.

In this work the formulated algorithm is benched marked with the 2d Ising model as a standard means of testing performance. The tests allow for a comparision to exact results and to previous benchmarks of other algorithms. The tests with the 2d Ising model also allow for insight in how to implement the algorithm to a materials science problem. The main goal in this work was to calculate the configurational energy density of states of the lithium ion conductor $Li_{0.5}La_{0.5}TiO_3$. This material is part of a family of possible stoiciometries $Li_{3x}La_{2/3-x}TiO_3$ of interest as solid state lithium ion conductors[14–20]. For all of the possible stoiciometries there is a tendency towards ordering of the lithium and lanthanum into lithium rich layers and lanthanum rich layers. The primary calculation of this work is that of the temperature dependant order parameter related to the lanthanum rich layer in $Li_{0.5}La_{0.5}TiO_3$. This calculation both serves to benchmark the application of the algorithm to a materials science problem with experimental knowns and to provide further insight into the physics of the material.

The rest of the article is organized as follows; a section explaining and motivating the new algorithm, a section bench marking the algorithm with the 2d ising model, then a section applying the algorithm to the $Li_{0.5}La_{0.5}TiO_3$ system followed by the conclusions.

ALGORITHM

The B_LENDER algorithm proposed in this work is given as follows. It is noted that the following algorithm is in terms of producing a relative density of states $G_r(E_j)^I$, where I is the iteration number.

1. $G_r(E_j)^I, \ \{\Sigma_s, e_s\}_{\mathcal{S}}^I$

2. $\{\Sigma_s, e_s\}_{\mathcal{S}}^I \rightarrow \{\Sigma_s', e_s'\}_{\mathcal{S}}^I$

3. $\Sigma_s'^I, e_s'^I \rightarrow \Sigma_s^{I+1}, e_s^{I+1} \ P = \ min[1, G_r(e_s)^I/G_r(e_s')^I]$

 $else \ \Sigma_s^I, e_s^I \rightarrow \Sigma_s^{I+1}, e_s^{I+1}$

4. $G_r(E_j)^{I+1} =$

$$G_r(E_j)^I + \frac{C_o \mathcal{H}(E_j, \{e_s\}_{\mathcal{S}}^{I+1})}{[\sum_j G_r(E_j)^I]^{\frac{1}{N}}} G_r(E_j)^I =$$

$$G_r(E_j)^I(1 + \frac{C_o \mathcal{H}(E_j, \{e_s\}_{\mathcal{S}}^{I+1})}{[\sum_j G_r(E_j)^I]^{\frac{1}{N}}})$$

$$(2)$$

Where $G_r(E_j)^0 \equiv [1 + \frac{C_o}{S} \mathcal{H}(E_j, \{e_s\}_{\mathcal{S}}^0)]$ with $\mathcal{H}(E_j, \{e_s\}_{\mathcal{S}})$ being a histogram function that counts the number of energies E_j in the set $\{e_s\}_{\mathcal{S}}$. In this work $\{\Sigma_s, e_s\}_{\mathcal{S}}^0$ is a randomly(uniformly) drawn set from the configuration space $\{\Sigma_i, e_i\}_{\Omega}$. In the second step a random change is applied to each element of the sampled set $\{\Sigma_s, e_s\}_{\mathcal{S}}^I$ to produced a "perturbed" set $\{\Sigma_s', e_s'\}_{\mathcal{S}}^I$, for the Ising model this could be randomly flipping a spin. In the third step a random number is drawn between zero and one for every sampled configuration, if this number is less then the ratio of the current density of states of the unprimed to primed energies $G_r(e_s)^I/G_r(e_s')^I$ then the perturbed configuration and energy $\Sigma_s'^I, e_s'^I$ goes to $\Sigma_s^{I+1}, e_s^{I+1}$, else the unperturbed configuration and energy Σ_s^I, e_s^I goes to $\Sigma_s^{I+1}, e_s^{I+1}$. This step (third) is dervied from the Wang and Landau method of sampling with probablity proportional to the inverse of the density of states. In the fourth step a histogram of the updated $\{e_s\}_{\mathcal{S}}^{I+1}$ energies is made and added (blended) into the current density of states $G_r(E_j)^I$ by multiplying by a constant C_o(which affects the convergence properties) and $G_r(E_j)^I$ divided by the sum of the density of states to the $1/N$ power. The $1/N$ power is introduced as tuning paramter to affect the convergence properties and was discovered through emprical testing with the 2-d Ising model. The fourth step is also shown in terms of multiplication which is discussed later. In this work it was found $C_o = \Omega^{\frac{1}{N}}$ was computationally efficient. After the algorithm is deemed to be complete it is necessary to re-normalize the iterated relative density of states $G_r(E_j)^f$ at the final iteration $I = f$ as follows,

$$1. \ A = \sum_j G_r(E_j)^f$$

$$2. \ G(E_j) \approx G_r(E_j)^f \frac{\Omega}{A},$$

$$(3)$$

to produce the properly normalized estimated value of $G(E_j)$. In principle the $G_r(E_j)$ can also be renormalized based on information of the number of configurations in

a given bin. For example if the ground state is known to have a given degeneracy then the entire density of states can be normalized such that the ground state bin has the corret degeneracy.

An important discussion point of this algorithm (Eq 2) is the update of the relative density of states(step four) being presented as addition and multiplication. In the addition form the self consistent nature of the update is clear, in the sense that the density of states is updated by adding a piece proportional to the counts in the histogram of the random set times the relative proportion of that energy level in the current estimate of the density of states. In the typical Wang and Landau sampling the update of the density of states is preformed by multiplication combined with a periodic reduction of the multiplication factor when a histogram of visited energies reaches a predetermined flatness criteria, the histogram of the visted energies is then reset to zero. In the multiplication form of step four of this algorithm (Eq 2) it is seen that the dependence on one over the sum of the density of states serves to naturally reduce the multiplication factor as the simulation progresses. The multiplication form is also useful when Ω is large and the sum of the density of states is larger than a typical floating point number. In this case the log of the density of states can be stored and the update performed through addition of logs. Taking $G_r^M \equiv max[G_r(E_j)]$ the log of $\sum_j G_r(E_j)^I$ can be written as,

$$
\begin{aligned}
G_r^{LS} &\equiv \log[\sum_j G_r(E_j)^I] = \log[G_r^M \frac{\sum_j G_r(E_j)^I}{G_r^M}] = \\
&\log[G_r^M] + \log[\sum_j e^{\ln[G_r(E_j)]-\ln[G_r^M]}] .
\end{aligned}
\tag{4}
$$

With G_r^{LS} from Eq 4 the log update form of step four of the algorithm (Eq 2) can be written as the following,

$$
\begin{aligned}
&\log[G_r(E_j)^I(1 + \frac{C_o \mathcal{H}(E_j, \{e_s\}_\mathcal{S}^{I+1})}{[\sum_j G_r(E_j)^I]^{\frac{1}{N}}})] = \\
&\log[G_r(E_j)^I] + \log[1 + \mathcal{H}(E_j, \{e_s\}_\mathcal{S}^{I+1})e^{\ln[C_o]-\frac{1}{N}G_r^{LS}}] .
\end{aligned}
\tag{5}
$$

In this form the alogrithm can be implemented even when Ω is large. To implement the ratio of the density of states in step two of the algorithm,

$$
e^{\ln[G_r(e_s)^I]-\ln[G_r(e_s')^I]} ,
\tag{6}
$$

can be used.

BENCH MARK WITH 2D ISING MODEL

In this work the algorithm discussed is tested using the 2d square zero field Ising model with lattice dimension of even number[21–23]. The configurations Σ_i and energies e_i of the 2d Ising model are inherently defined by the lattice site spin variables and coupling constant J. The first test is of the effectiveness of the algorithm in calculating the density of states of the 2d ising model. To test the accuracy of the simulations the results will be compared to the exact result solved by Beale [24]. The accuracy of the simulation will be determined by the error defined as,

$$
\begin{aligned}
\mathcal{E}(I,o) &= < |\epsilon(E_j, I, o)| >_j \\
&= \frac{1}{\Pi} \sum_{j=1}^{\Pi} \frac{|\ln(G_{ex}(E_j)) - \ln(G_r(E_j, I, o))|}{|\ln(G_{ex}(E_j))|} .
\end{aligned}
\tag{7}
$$

Where $G_{ex}(E_j)$ is the exact density of states, $G_r(E_j, I, o)$ is the calculated density of states at iteration number I from initial conditions and trajectory o, and $|\epsilon(E_j, I, o)|$ is the absolute value of the fractional error for a specific energy level. In Eq 7 the relative density of states $G_r(E_j, I, o)$ is renormalized according to Eq 3 prior to calculation of the error. The primed configurations in this work were generated by randomly flipping one spin on the Ising lattice

This first test of the algorithm is with the 32X32 Ising model. In a materials science problem with first principles calculations the system size is not expected to be anywhere near the size of the 32X32 Ising model so these results are included to show the algorithm may have potential for larger system size. While the ideal value of N is not known prior to the calculation it was found in this work that a value of $N = 0.1$ was computationally efficient for the 32X32 Ising model. In Fig 1 the value of the average error calculated with Eq 7 is shown up to 1e7 iterations for $S = 1$, 10, 100, 1000, and 1e4. The data in Fig 1 is averaged over 36 individual simulations for each value of S. The results show linear scaling from $S = 1$ to $S = 10$ and then another order of magnitude improvement from $S = 10$ to $S = 1000$, no significant improvement is discernable going to $S = 1e4$. The periodic flucuations in the avgerage error are also noted in going to larger S, it is hypothesized that these fluctions are related to the tunneling time of the walkers. The results at $S = 1000$ show that the average error is comparable to a linear speed up of the error reported for a single random walker in the orignial Wang and Landau algorithm. Defining a effective Monte Carlo step defined here as,

$$
MC = \frac{S \times I}{\Pi} ,
\tag{8}
$$

where Π is the number of energies. For $S = 1000$, with the number of energies for the 2-d Ising model given by $n \times n$, at $I = 1e7$ gives $MC \approx 1e6$. With the value of the average error being $< 0.1\%$ for $S = 1000$ at $MC \approx 1e6$ the B$_L$ENDER algorithm is performing very

well in terms of parallel speed up as compared to the reports for the orignial Wang and Landau algorithm for a single Walker[6]. In comparison a single walker ($\mathcal{S} = 1$) simulated to $MC = 1e6$ using $N = 0.1$ has an average error of $\approx 0.2\%$, where the result is averaged over 36 independant calculations.

In Fig 1b are also the results for the average error of 36 independant simulations for a 10×10 Ising model for the different number walkers $\mathcal{S}$ with $N = 1$. The results show that the scaling is quite good as the number of walkers increases. This result is encouraging becuase the number of configurations that will be typical for a supercell approximation in a first principles calculation is not expected to exceed the large number of $\approx 10^{30}$ configurations in the 10×10 Ising model. This test on the smaller model indicates the algorithm is suitable for implementation in the materials science problem tackled in this paper.
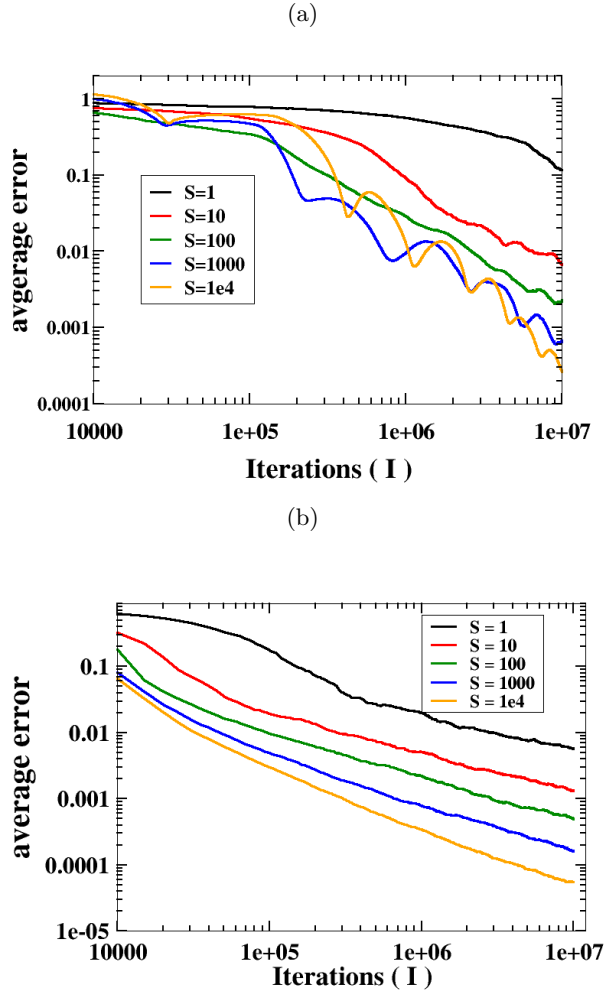
(a)

(b)

FIG. 1. Average error from 36 simulations calculated from Eq 7 with $\mathcal{S} = 1$, 10, 100, 1000, and 1e4 for (a) the 32×32 Ising model with $1/N = 0.1$, (b) the 10×10 Ising model with $1/N = 1$.

Another aspect of the algorithm to consider is the dependence on the value of N and of C_o. In Fig 2 the dependence on N is shown for the 32X32 and 10X10 Ising models, simulated to $I = 1e7$ and $I = 1e6$ respectively, with $\mathcal{S} = 100$, and averaged over 36 independant calculations. The results show that for the larger 32X32 model the dependence on N is more pronounced and that the optimal value of N is lower than for the smaller 10X10 model. The more pronounced convergence dependence on N for the larger 32X32 model does pose a problem if one was to implement the the algorithm for a new system where the density of states is not known beforehand becuase there is no current evidence to predict what the optimal paramter would be. The tests with the 10X10 model suggest that for a smaller system size that the convergence dependence on N is less pronounced and that $N = 1$ is sufficient. The results presented here suggest that if one was to use the algorithm for a larger system size some method of predicting the optimal value of N would be required. These tests have used a value of $C_o = \Omega^{1/N}$, this value was based on tests showing this to be an optimal value. In Fig 3 is shown the error for a 10×10 Ising model vs $C_o/\Omega^{1/N}$ with $N = 1$ simulated to 1e7 iterations averaged over 36 independant runs. The results in Fig 3 show that the optimal value of C_o is at $\Omega^{1/N}$.
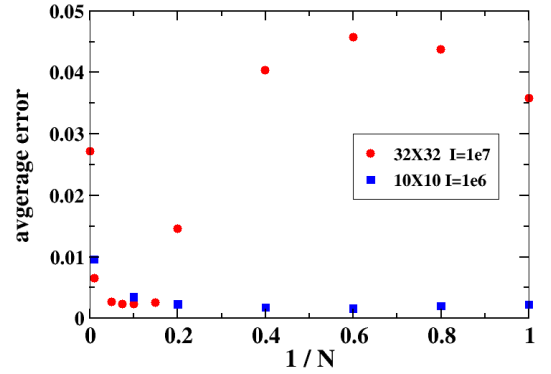

FIG. 2. Average error from 36 simulations calculated from Eq 7 vs the value of $1/N$ for the 32×32 Ising model simulated to 1e7 iterations as red circles and the 10×10 Ising model simulated to 1e6 iterations as blue squares.

Relationship of the B_LENDER algorithm to the N-fold 1/t algorithm

In the introduction is was mentioned that an improvement to update of the Wang and Landau method had been made by Belardinelli et al. [12], which was referred to as the 1/t algorithm. It was found in this work that for the $\mathcal{S} = 1$, $N = 1$, and $C_o = \Omega$ that the B_LENDER
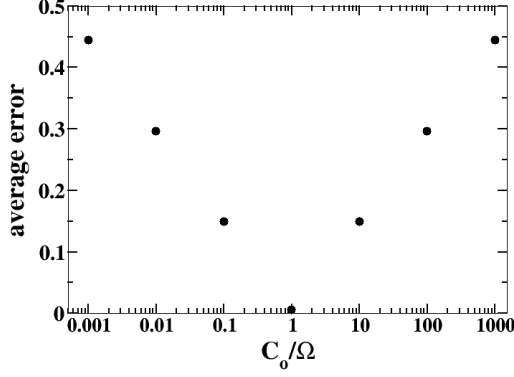
(a)

FIG. 3. Average error from 36 simulations calculated from Eq 7 for the 10×10 Ising model with $1/N = 1$ vs the value of C_o.

algorithm had similar behavior to the results of Belardinelli et al.. To make the comparision we first note that in the multiplication form of the B_LENDER algorithm we can define,

$$f(I) \equiv (1 + \frac{\Omega\mathcal{H}(E_j, \{e_s\}_{\mathcal{S}=1}^{I+1})}{[\sum_j G_r(E_j)^I]}) \qquad (9)$$

such that the update to the density of states is given by,

$$G_r(E_j)^{I+1} = G_r(E_j)^I f(I) . \qquad (10)$$

This is in the original form of the Wang and Landau Algorithm the difference being how $f(I)$ changes with time(iteration). In the work by Belardinelli et al. They defined a value $F(t) = \log(f(t))$ and found an optimal form of $F(t) = \frac{c}{t^p}$, with $t = MC$ as defined by Eq 8. They found the optimal values to be $c = 1$ and $p = 1$. They also described a more complex variant of this algorithm called the N-fold 1/t that incoporated the average life time of the initial configurations. In their work they used a 8×8 Ising model, so to compare, calculations of the average of $F(t)$ and the error defined by Eq 7 from 36 simulations was done for the B_LENDER algorithm. The results for the average value of $F(t)$ are shown in black in Fig 4(a) and the average error in Fig 4(b). In comparing the results to those from Fig 5 of Belardinelli et al. [12] shown in red in Fig 4, a striking similarity is seem in the behavior as compared to the N-fold 1/t algorithm. It is clear from this comparision that there is a mathematical relationship between these two algorithms although at the moment the exact nature of this relationship is unclear. To further analyze the results of Fig 4(a) it is noted that assuming $F(t) = \frac{c}{t^p}$ a linear fit of $\log F(t)$ vs $\log(t)$ will predict the coefficients c and p. Fitting the results from the B_LENDER algorithm in Fig 4(a) in this manner gives $c = 1.8$ and $p = 1$. So the value of p is found to be in agreement with that of Belardinelli et al.
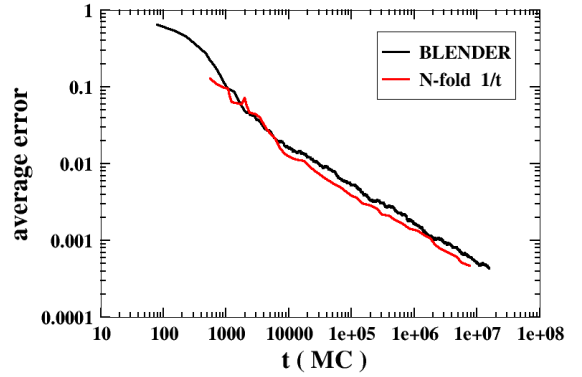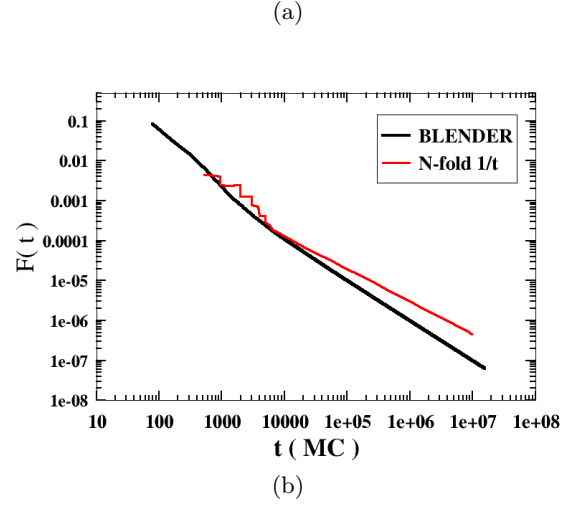
(a)

(b)

FIG. 4. In black (a) The average of $F(t)$ and (b) the average error defined by Eq 7 for 36 simulations of the 8×8 2-d Ising model with the B_LENDER algorithm with $\mathcal{S} = 1$, $N = 1$, and $C_o = \Omega$. In red (a) $F(t)$ results taken from the work of Belardinelli et al. [12] (b) the error defined by Eq 7 taken from the work of Belardinelli et al.. Here $t = \frac{I}{64}$ or equivalently one Monte-Carlo time step (MC) as defined by Eq 8.

while c is marginally larger. These similarities with the N-fold 1/t algorithm, which is proven to be convergent, give further confidence in the B_LENDER algorithm and suggest it is likely to be convergent as well.

APPLICATION TO LLTO

The purpose of developing the B_LENDER algorithm was to develop and algorithm suitable for the needs of solid state density functional theory calculations of disordered lattice materials. Due to the long run time of density functional theory calculations the parallel nature of B_LENDER allows for calculations of each energy to be done as independant job submissions to a computer cluster. The results can then be processed by a script running on the head node. In this work the B_LENDER algo-

rithm is applied to the lithium and lanthanum sub lattice of the solid state lithium ion electrolyte $Li_{0.5}La_{0.5}TiO_3$. The goal of this study was to both, perform a calculation with B_LENDER of a real material system that is fairly well understood, and also to learn something new in the process. Specifically the desired knowledge to be gained is a better understanding the disordering of the lithium and lanthanum sub lattice and associated lattice distortions.

Background on LLTO

LLTO is a complex material comprised of a variety of stoiciometries and phases but in this work the study is restricted to the reported tetragonal P4mmm phase of the stoiciometry $Li_{0.5}La_{0.5}TiO_3$[15, 19]. A unit cell of this structure is shown in Fig 5. The lattice parameters for this unit cell were taken from the experimental results from Ibarra et al.[15]; 3.8688(4)$\mathring{A}$ for a and b axes, and 7.7463(2) for c-axis. This unit cell is representative of an ordered form of $Li_{0.5}La_{0.5}TiO_3$ where the lithium and lanthunum are seperated into seperate layers on the high symettry A-sites. Where the A-site refers to the general pervoskite formula unit ABX_3. The structure in Fig 5 is actually strucutrally unstable and the energy can be lowered by lattice disortions which manifests as tilts in the titaninum oxygen octehedra and the lithium and lanthum distorting off of the high symettry A-sites. The instablity of the structure in Fig 5 is evidenced by the imaginary phonon modes calculated by Moriwake et al. [16].

The physics of interest in this study is to understand the disordering of lithium and lanthanum between layers. It is reported for this phase that the lanthanum are mostly mixed between layers when the samples are slow cooled during synthesis and if quenched from high temperature the lanthanum ordering is reported to be completely mixed between layers [15]. Apart from the mixing of lithium and lanthum between layers there is also configurational complexity associated with octahedral tilting. In this work the B_LENDER algorithm is used to evaluate the density of configuration states associated with local minium corresponding to both the litihium and lanthanum ordering and lattice distortions.

Computational Details

In this work a 3×3×1 supercell of the unit cell shown in Fig 5 was used as an approximation to bulk $Li_{0.5}La_{0.5}TiO_3$. While not an ideal size as it is still restrictive of the possible lattice configurations and to the types of domains of octehedral tilting that can form it is
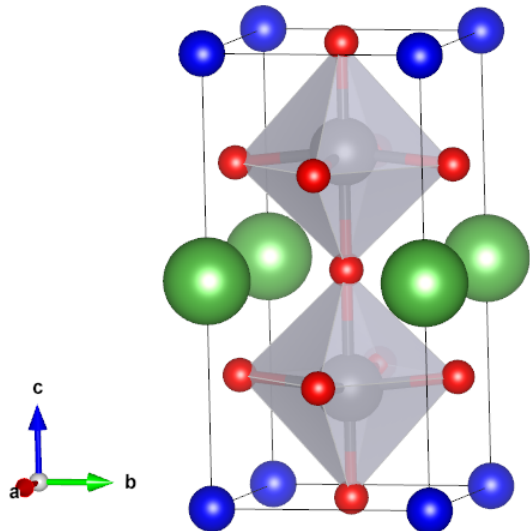

FIG. 5. 10 atom unit cell of P4/mmm $Li_{0.5}La_{0.5}TiO_3$. Where dark blue spheres are lithium, green spheres are lanthanum, red spheres are oxygen, and grey spheres inside of octahedra are titanium.

the largest supercell practical for performing the configurational Monte-Carlo in this work.

An important aspect of completing this study is a scheme for producing the initial and primed configurations in the iterative process of the B_LENDER algorithm. The scheme used in this study was to first generate a set of lithium and lanthanum randomly placed on the high symettry A-sites where occupancy is restricted to one, then a small amount of noise on the order of $\pm 0.2\mathring{A}$ was added to each lithium and lanthanum coordinate. These configurations were then relaxed to a local minimum which formed the first set of configurations in the iterative process. Then the primed configurations (step 2) were formed by swapping a random lithium and lanthum atom and placing them back on the high symmetry A-site along with a new amount of random noise, these configurations where then relaxed to a local minimum. The random noise off the A-site served to allow for searching the distorted lattice configuration space.

The methods used in the calculation of the total energies of the lattice configurations of LLTO in this work was density functional theory using the VASP code[25–28] within the projector augmented wave formalism[29]. The PBE variant of generalized gradient approximation was used for the exchange and correlation functional[30]. The valence electron configurations for the data sets were; $5p^65d^16s^2$ for La, $2s^1$ for Li, $3p^63d^23s^2$ for Ti, and $2s^22p^4$ for O. The calculations also took advantage of the "soft" option for La and O. The total energy cut off for expansion of the plane waves was 250 eV. Self consistent cycles were converged with a energy difference of < 2.5e-

5 eV and relexation of atomic coordinates was terminated when the difference in total energy between ionic relaxation steps was < 2.5e-4 eV. A 1X1X2 gamma centered k-point mesh was used for the 3X3X1 supercells of the LiLaTiO6 unit cell. These cut offs and parameters were choosen to maximize compuatational efficiency while retaining enough accuracy to capture important physical properties of LLTO. To test the accuracy of these methods 10 structures were calculated with fixed coordinates at these convergence criteria and more accurate PAW data sets and cutoffs. The more accurate PAW datasets included the valence electron configurations; $5s^2$, $5p^65d^16s^2$ for La, $1s^22s^1$ for Li, $3p^63d^23s^2$ for Ti, and $2s^22p^4$ for O. The cutoffs for the more accuracte calculations were 450eV for the plane wave basis, and 2X2X3 gamma centered k-points. The average magnitude of the error in relative energy between structures from this test was 0.05 eV.

The calculations were performed at the experimental lattice paramaters $3.8688\mathring{A}$ for a and b axes, and 7.7463 for c-axis. The paramaters for the B_LENDER algorithm were $\mathcal{S} = 10$ and $N = 1$. The bin width used for determining $G_r(E_j)$ was choosen to 0.02eV. The value of omega was estimated as 100 times the combinatoric number of configurations of the lithium and lanthanum ordering onto the A-site given as,

$$\Omega \approx 100\frac{18!}{9!9!} \ . \tag{11}$$

While an exact value of Ω is not needed for the algorithm to converge experience suggests that being close as possible is computationally beneficial. Estimating that Ω is greater than the combinatoric calculation of the lithium and lanthanum in the A-site cages comes from the possibility of multiple distinct lattice distortions for each type of A-site cage configuration.

Results

Using the paramters and configurational enumeration scheme specified above a simulation was performed to 3000 iterations for the 3×3×1, 90 atom supercell. After 150 iterations the algorithm was restricted to look in the energy range less than 1.25eV higher than the lowest energy found at that time. This was to improve compuatational efficiency by preventing the walkers from exploring an unnecessarily high energy range. While 3000 iterations is not ideally converged, it was sufficient to gain further understanding of the material. It is expected that the qualititave aspects of the results are well accounted for despite the limited number of iterations.

The main focus of the results is the nature of the lithium and lanthanum sublattice ordering. To accomplish this the order parameter of interest is that of the occupancy of lanthanum in the lanthanum rich layer along the c-axis. In the work by Ibarra et al. [15] they refer to this order paramater as $La1$, the same convention will be used in this work. This order paramter $La1$ is defined as the number of lanthanum in the lanthanum rich layer divided by the total number that could occupy the layer. As an example the unit cell in Fig 5 woud have $La1 = 1$. It is important to note in this work the 3×3×1 supercell restricts the configurations along the a and b axis from having altenerate layering of lithium and lanthanum rich layers. Ideally the calculations would be done with at least a 4×4×1 supercell but the computational effort is beyond the scope of this work. The results later will have to be interpreted taking this systematic supercell error into account.

To calculate the ensemble average of these order paramaters first arithmetic averages of the order parameter at each energy level E_j are calculated from the primed configurations ($\{\Sigma_s^{'}\}$) that occurred during the simulation. The arithmetic average of a general order parameter O over all configurations with energy E_j is denoted by $< O >_j$. Then with these the ensemble average is computed as,

$$\langle O \rangle = \sum_{j=1}^{\Pi} < O >_j G_r(E_j)\frac{e^{-\frac{E_j}{k_BT}}}{Z} \ . \tag{12}$$

Where $Z = \sum_{j=1}^{\Pi} G_r(E_j)exp(-\frac{E_j}{k_BT})$. It is noted that normalization of the relative density of states to the appropriate number of configurations is not necessary for the calculation of the ensemble average of an order parameter. If wanting to compare free energies($-k_BT\ln(Z)$) between phases it would be necessary to normalize the density of states properly to obtain an accurate calculation of the free energy.

The first main result to report is a view of the convergence of $G_r(E_j)$ as a function of the iterations. In Fig 6 $G_r(E_j)$ is shown at $I = 500$, 1000, and 3000 with the y-axis plotted on a log scale. The $G_r(E_j)$ shown in Fig 6 are plotted such that the lowest energy of $G_r(E_j)$ found at the particular iteration shown is set to zero, the sharp cutoff at higher energy was the upper limit to configurational search, and the plots are normalized by dividing through by the minimum of $G_r(E_j)$ at that iteration. The main characteristic of the results by 3000 iterations is the presence of some low energy states with a energy gap up to a more continous spectrum of states. The lowest energy configuration is characterized as having $La1 = 1$, that being having alternate layers of lithium and lanthanum along the c-axis. It is not however equivelent to the unit cell shown in Fig 5, in that the structures have distinct lattice disortions.

The next result is the arithmetic averages of the $La1$ order parameter which is shown in Fig 7a along with the number of samples used to determine each value in Fig 7b. The results in Fig 7a show an over all tendency for
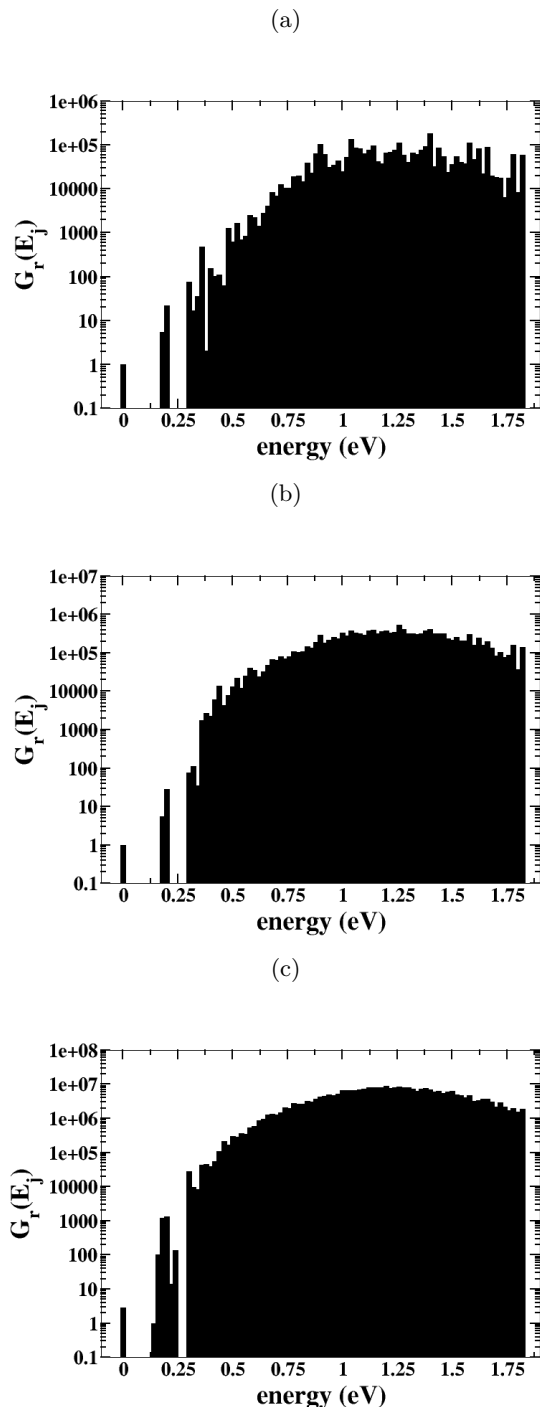
(a)

(b)

(c)

FIG. 6. Plots of $G_r(E_j)$ at (a) 500 iterations, (b) 1000 iterations, and (c) 3000 iterations. The plots are normalized by dividing through by the smallest value of $G_r(E_j)$ at that particular iteration. The plots are shown with a log scale on the y-axis.

more mixing of La and Li between layers for higher energies. The ensemble average of $La1$ is shown in Fig 8 which shows a phase transition from completely segregated Li and La between layers to mostly mixed between

layers and increased mixing with increasing temperature. For the $3 \times 3 \times 1$ model the minimum possible value of $La1$ is $5/9 = 0.56$. These results are in qualitative agreement with expriment and it is expected that that larger supercell models would increase the available configurational entropy and result in a reduced value of $La1$ in the disordered phase.

To analyze the convergence of the 3000 iterations an inspection of the flatness of the histogram of energies of the visited configurations can be done. The visited configurations are defined by step 3 of Eq 2. The histogram of the visited energies during the simulation are shown in Fig 10. The results show that the histogram is qualitatively flat for ≥ 0.5eV. This result along with the counts for calculating the $La1$ order parameter shown in Fig 7(b) suggest that the results are most well converged for ≥ 0.5eV. In this sense the statement can be made that the strongest result of this computation is the trend for more mixed configurations to have higher energy seen in the range ≥ 0.5eV. While the first principles methods used can be considered coarsed grained in terms of PAW data sets, total energy cutoffs, and k-points as observed from testing with more accuracate methods it is expected that some error cancelation is present such that the overall trend seen in Fig 7(a) is still qualitatively correct. It must be said that the ensemble average of $La1$ is highly dependant on the low energy structures as per the exponential nature of the parition function. In this regard the observed phase transition in Fig 8 can not be expected to be an accuracte prediction of a transition temperature. The most important result of Fig 8 is the high temperature region above the phase transition showing a tendency for greater mixing of Li and La for increasing temperature.

To gain some further insight in to the structures found during the search the two lowest energy strucutures are shown in Fig 9 (a) and (b). In Fig 9 (a) it is seen that the lowest energy structure has the Li and La completely segregated between layers along the c-axis. In Fig 9 (b) that the second lowest energy structure has a fully occupied layer of Li along the a-axis along with two paritially occupied layers. Due to the psuedo cubic nature of the system it is expected that there would be neary energetically identical structures of consisting of compeletely segregated Li and La layers along the a and b axes. This feature of ambiguity of the orientation of how the Li and La rich layers can form are a likely driving force for the numerous domain boundaries observed in experiments for other stoiciometries synthezied by annealing from high temperature. Due to the $3 \times 3 \times 1$ used in this study these structures were not possible to realize in the simulation but as evidenced by Fig 9 (b) segration of the Li and La into seperate layers is still energetically favorable. A common feature of both Fig 9 (a) and (b) is the Li sitting off of the high symettry A-site near the oxygen windows seperating A-site cages. This feature
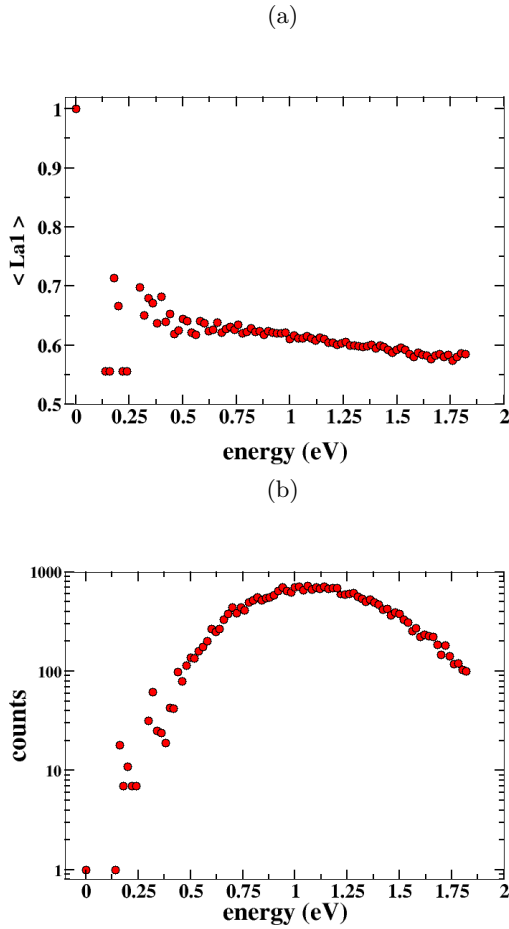
(a)

(b)

FIG. 7. (a) Arithmetic averages of La1 order parameter as a function of energy. (b) Number of counts to determine each value of the order paramater for each energy.

has been previously reported experimentally and theoretically in the literature[16, 20, 31].

Conclusions

This work has presented a parralel variant of the Wang and Landau algorithm refered to as B_LENDER($B_L$end Each New Density Each Round). The algorithm was developed purposely for use with disordered crystal sublattices and is naturally parallel. Its design makes it facile to implement on a mid level high performance computer such as BEBOP where individual jobs can be submitted to compute nodes independently and managed by a script running on a head node. It was trialed using the 2-d Ising model and showed good performance as compared to pervious reports of the Wang and Landau algorithm. In the case of using one walker the B_LENDER algorithm was also found to have similar behavior as to the N-fold 1/t algorithm of Belardinelli et al.. Knowledge gained from testing with the 2-d Ising model al-
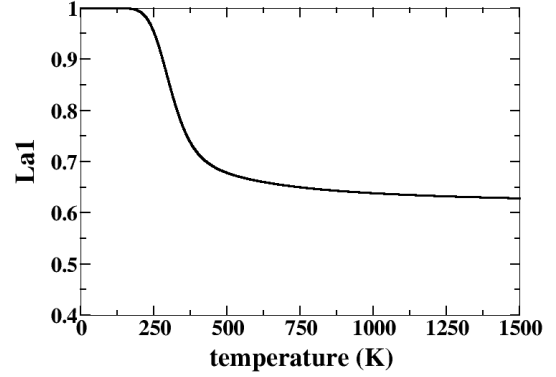

FIG. 8. Ensemble average of La1 order parameter calculated with Eq 12 as function of temperature.
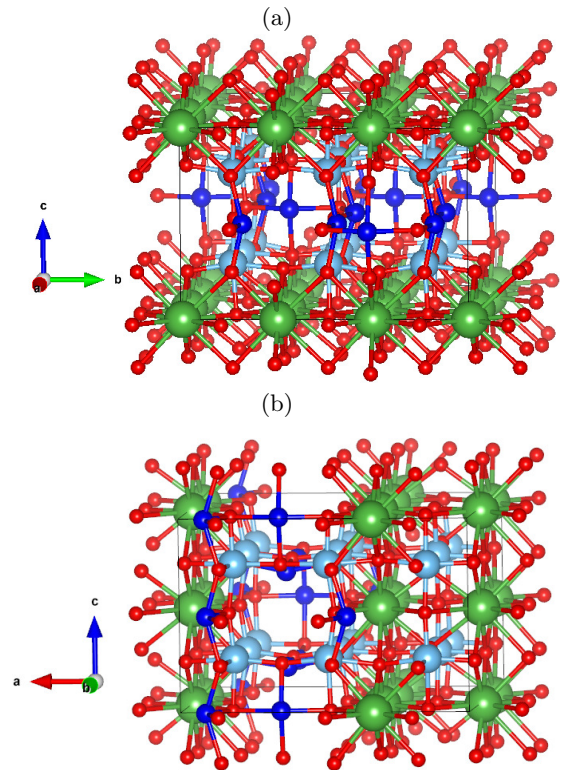

(a)

(b)

FIG. 9. Low energy structures found during simulation

lowed for an imformed implentation to the real material science problem of studying the Li and La sublattice disorder of $Li_{0.5}La_{0.5}TiO_3$ using density functional theory methods. While simulation cell size and total number of iterations were not ideal for a highly accuracte calculation they non the less were consistent with experimental knowledge and provided additional insight into the disordered nature of the material. It was found that lower energy structures favored segrating Li and La into seperate layers and that structures with Li and La
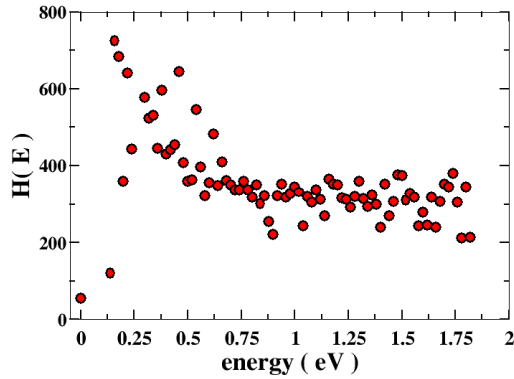
FIG. 10.

mixed between layers were on average higher in energy than more segrated structures. Thermodynamic analysis of the order parameter related Li and La intermixing between layers showed at phase transition between completely segragated to mostly mixed tending to more mixed at higher temperatures. Overall the results show that the algorithm performed well in simulating both the 2d Ising model and with first princples calculations of a real material system.

[1] W. Kohn and L. J. Sham. Self-consistent equations including exchange and correlation effects. *Phys. Rev.*, 140:A1133–A1138, 1965.

[2] N. Metropolis, A. W. Rosenbluth, M. N. Rosenbluth, A. H. Teller, and E. Teller. Equation of state calculations by fast computing machines. *J. Chem. Phys.*, 21(6):1087–1092, 1953.

[3] D. P. Landau and K. Binder. *A Guide to Monte Carlo Simulations in Physics*. Cambridge University Press, fourth edition edition, 2015.

[4] Bernd A. Berg and Thomas Neuhaus. Multicanonical ensemble: A new approach to simulate first-order phase transitions. *Phys. Rev. Lett.*, 68:9–12, Jan 1992.

[5] Jooyoung Lee. New monte carlo algorithm: Entropic sampling. *Phys. Rev. Lett.*, 71:211–214, Jul 1993.

[6] F. Wang and D. P. Landau. Efficient, multiple-range random walk algorithm to calculate the density of states. *Phys. Rev. Lett.*, 86:2050–2053, Mar 2001.

[7] J. Yin and D. P. Landau. Massively parallel wanglandau sampling on multiple gpus. *Comput. Phys. Commun.*, 183(8):1568 – 1573, 2012.

[8] L. Zhan. A parallel implementation of the wanglandau algorithm. *Comput. Phys. Commun.*, 179(5):339 – 344, 2008.

[9] T. Vogel, Y. W. Li, T. Wüst, and D. Landau. Generic, hierarchical framework for massively parallel wang-landau sampling. 110:210603, 05 2013.

[10] M. Eisenbach, D. M. Nicholson, A. Rusanu, and G. Brown. First principles calculation of finite temperature magnetism in fe and fe3c. *Journal of Applied Physics*, 109(7):07E138, 2011.

[11] S. N. Khan and Markus Eisenbach. Density-functional monte-carlo simulation of cuzn order-disorder transition. *Phys. Rev. B*, 93:024203, Jan 2016.

[12] R. E. Belardinelli and V. D. Pereyra. Wang-landau algorithm: A theoretical analysis of the saturation of the error. *The Journal of Chemical Physics*, 127(18):184105, 2007.

[13] Chenggang Zhou and Jia Su. Optimal modification factor and convergence of the wang-landau algorithm. *Phys. Rev. E*, 78:046705, Oct 2008.

[14] Xiang Gao, Craig A. J. Fisher, Teiichi Kimura, Yumi H. Ikuhara, Akihide Kuwabara, Hiroki Moriwake, Hideki Oki, Takeshi Tojigamori, Keiichi Kohama, and Yuichi Ikuhara. Domain boundary structures in lanthanum lithium titanates. *J. Mater. Chem. A*, 2:843–852, 2014.

[15] J Ibarra, A Vrez, C Len, J Santamara, L.M Torres-Martnez, and J Sanz. Influence of composition on the structure and conductivity of the fast ionic conductors la2/3xli3xtio3 (0.03x0.167). *Solid State Ionics*, 134(3):219 – 228, 2000.

[16] Hiroki Moriwake, Xiang Gao, Akihide Kuwabara, Craig A.J. Fisher, Teiichi Kimura, Yumi H. Ikuhara, Keiichi Kohama, Takeshi Tojigamori, and Yuichi Ikuhara. Domain boundaries and their influence on li migration in solid-state electrolyte (la,li)tio3. *Journal of Power Sources*, 276:203 – 207, 2015.

[17] H.X. Geng, A. Mei, C. Dong, Y.H. Lin, and C.W. Nan. Investigation of structure and electrical properties of li0.5la0.5tio3 ceramics via microwave sintering. *Journal of Alloys and Compounds*, 481(1):555 – 558, 2009.

[18] Anatolii Belous, Oleg Yanchevskiy, Oleg V'yunov, Odile Bohnke, Claude Bohnke, Franoise Le Berre, and Jean-Louis Fourquet. Peculiarities of li0.5la0.5tio3 formation during the synthesis by solid-state reaction or precipitation from solutions. *Chemistry of Materials*, 16(3):407–417, 2004.

[19] S. Stramare, V. Thangadurai, and W. Weppner. Lithium lanthanum titanates: a review. *Chemistry of Materials*, 15(21):3974–3990, 2003.

[20] Michele Catti. First-principles modeling of lithium ordering in the llto (lixla2/3-x/3tio3) superionic conductor. *Chemistry of Materials*, 19(16):3963–3972, 2007.

[21] R. J. Baxter. *Exactly Solved Models in Statistical Mechanics*. Elsevier, 2016. ISBN 978-0-12-083180-7.

[22] L. Onsager. Crystal statistics. i. a two-dimensional model with an order-disorder transition. *Phys. Rev.*, 65:117–149, 1944.

[23] B. M. McCoy and T. T. Wu. *The Two-Dimensional Ising Model*. Harvard University Press, 1973.

[24] P. D. Beale. Exact distribution of energies in the two-dimensional ising model. *Phys. Rev. Lett.*, 76:78–81, Jan

1996.

[25] G. Kresse and J. Hafner. Ab initio molecular dynamics for liquid metals. *Phys. Rev. B*, 47:558–561, Jan 1993.

[26] G. Kresse and J. Hafner. Ab initio molecular-dynamics simulation of the liquid-metal–amorphous-semiconductor transition in germanium. *Phys. Rev. B*, 49:14251–14269, May 1994.

[27] G. Kresse and J. Furthmller. Efficiency of ab-initio total energy calculations for metals and semiconductors using a plane-wave basis set. *Computational Materials Science*, 6(1):15 – 50, 1996.

[28] G. Kresse and J. Furthmüller. Efficient iterative schemes for ab initio total-energy calculations using a plane-wave basis set. *Phys. Rev. B*, 54:11169–11186, Oct 1996.

[29] P. E. Blöchl. Projector augmented-wave method. *Phys. Rev. B*, 50:17953–17979, Dec 1994.

[30] J. P. Perdew, K. Burke, and M. Ernzerhof. Generalized gradient approximation made simple. *Phys. Rev. Lett.*, 77:3865–3868, Oct 1996.

[31] Xiang Gao, Craig A. J. Fisher, Teiichi Kimura, Yumi H. Ikuhara, Hiroki Moriwake, Akihide Kuwabara, Hideki Oki, Takeshi Tojigamori, Rong Huang, and Yuichi Ikuhara. Lithium atom and a-site vacancy distributions in lanthanum lithium titanate. *Chemistry of Materials*, 25(9):1607–1614, 2013.